

An Identification Problem for an Elastic Beam With Moving Load *

Ram Rajagopal, Alexander B. Kurzhansky and Pravin Varaiya
University of California at Berkeley, CA 94720-1770, USA
{ramr,kurzhans,varaiya}@eecs.berkeley.edu

October 22, 2008

1 Introduction

Weighing stations along the highway are used to check truck weights. These stations require separate areas along the highway where trucks stop to be weighed. Due to their high cost and also operational issues, such as requiring trucks to reduce speed and queue up for some time, such stations are scarce. In Weight In Motion Stations (WIM) trucks can be weighed as they slowly move along [2]. This technology is deployed in roadside weighing stations as a replacement to traditional weigh-in stations.

Traditional stations use bending plate, piezoelectric, or load cell sensors to measure the vertical forces applied by axles to sensors [2]. The stations require a controlled environment and continuous calibration to reliably estimate static axle loads. Additional calculations are then performed to transform the static axle load estimates into the dynamic load that the pavement actually experiences. The latter calculations are based on models of vehicle-pavement interactions. These interaction models are rarely if ever calibrated for individual WIM stations. [10, 24]

This paper explores a very different approach. The system comprises a network of sensor nodes (SN) and an access point (AP). Each SN assembles a single- or double-axis MeMS accelerometer, a microprocessor, flash memory, a radio, and an electronic PC board that interconnects these components. A pair of AA batteries powers the assembly. The SN is encased in a 3" 'Smart Stud' and glued on the pavement surface. The processed data are sent by the SN radio to the AP, situated on the side of the road. The AP may record the data locally or forward them to a remote site.

The SNs directly measure the vibration (acceleration) of the pavement under them. It may also be possible to process the SN data to estimate the truck axle weight and spacing, classification, and speed. The SN and AP used, together with the installation cost, are a fraction of the cost of current WIM stations.

Figure 1 shows a possible deployment.

[19] and [16] deal with a similar problem. But the application is restricted to bridges, and the model does not consider transient pavement effects. The models are much simpler since they

*Research supported by California Department of Transportation and ARO-MURI UCSC-W911NF-05-1-0246-VA-09/05

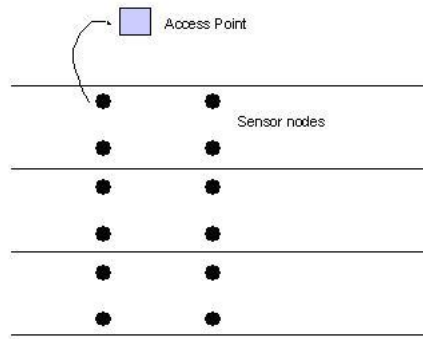


Figure 1: Deployment of proposed WIM system on a multi-lane freeway or bridge location. The sensor nodes are only 3" in diameter; the access point is a 5" cube. Data from sensors nodes are sent to the access point via radio. The sensor nodes and access points are drawn at an exaggerated scale relative to lane width.

rely on modal estimation, and give no accuracy guarantees. In bridges the responses have higher amplitudes as well as the decay is slower, making it possible for a modal estimation procedure to work. But among the many constraints, only a single truck at a time can pass through the bridge, which makes it an impractical solution.

We in turn, develop a different approach. We start our study with the analysis of a literature validated PDE model of the pavement [23, 12, 2]. We compute a closed form solution for the pavement response under truck motion. We then design optimal weight estimation algorithms using the closed form solution. Along the way we discuss issues such as required precision for SN, energy consumption for stand alone operation and communication requirements, as well as efficient algorithmic implementations.

The paper also holds independent interest due to the closed form solution derivation presented. To our knowledge no similar derivations exist in the literature for the situation presented. One advantage of the closed solution in the present case is that for usual parameters the system is stiff, and simulation poses serious difficulties. We attempted using some popular PDE solvers for computing the solution and obtained poor approximations.

Furthermore, our estimation problem aims at estimating a finite parameter, from infinite measurements or point measurements of an distributed dimensional system, contributing to the literature on estimation in systems described by partial differential equations [9, 6, 1, 17].

The paper is organized as follows. Section 2 states the pavement model and the estimation problem of interest. Section 3 develops an analysis of the model, including a closed form approximation that is of independent interest. In Section 4 we present methods for estimating the load under various setups. The presented method is optimal and can be used to gauge other methods used in practice. Section 5 introduces some system design considerations, regarding sensor placement and estimation methods. We discuss simulation results using real world pavement parameters in Section 6. The proofs of all theorems of the paper are presented in Section 7. Concluding remarks are presented in Section 8.

2 Problem statement

We consider the model of a road as an Euler beam with elastic foundation with a moving load. The vertical non-stationary force acting on the the road (beam) is due to transient dynamic loads applied through tires of moving vehicles [13, 18, 23].

The conventional *model of the equation of motion* of a one-dimensional damped beam is [see [2, 7, 12, 22]]

$$EI \frac{\partial^4 y}{\partial x^4} + \gamma \frac{\partial^2 y}{\partial t^2} + \kappa \frac{\partial y}{\partial t} + \beta y = F(x, t). \quad (1)$$

Here x and $y(x, t)$ are the horizontal position (along the road) and the vertical displacement (of the pavement), and $F(x, t)$ is the applied force at position x and time t . The displacement y varies in the domain $y \in R$, and the position x varies within the interval $[0, L]$. The standard road beam model makes the assumption $\beta > \kappa$, which results in the road pavement having natural frequencies [25].

The basic force resulting from a truck moving at velocity V is modeled as the *moving excitation*[13]

$$F(x, t) = F \cos(\omega_0 t) \times \delta(x - Vt), \quad (2)$$

where V is the velocity of the point of application of the force $F \cos(\omega_0 t)$ with magnitude F and frequency ω_0 . The magnitude and frequency are determined by the vehicle's suspension system. Typical values are $F = 50000 \text{ N}$ and $\omega_0 = 2\pi f_0$, where f_0 is between 1 Hz and 3 Hz [8, 5]. Real trucks have force excitations composed of a linear combination of basic components

$$F(x, t) = P(t) \times \delta(x - Vt), \quad (3)$$

$$P(t) = F \left(\sum_{r=0}^W P_r \cos(\omega_r t) \right),$$

where the number of components W and the frequencies ω_i depend on the truck suspension system type. For quarter car models, $W = 2$, $\omega_0 = 0$, ω_1 is in the given range [5, 24]. For walking beam models, $W = 3$, with $\omega_0 = 0$ [24]. The values of P_r are usually assumed to be equal or have a fixed proportion.

We also consider a *fixed excitation* applied at a point x_0 at time t_0

$$F(x, t) = F \delta(t - t_0) \delta(x - x_0), \quad (4)$$

The point of application of the force at time t is $x_a = Vt$. It starts to move at time $t_0 = 0$, from position $x_a(0) = 0$. This model is an approximation of the standard quarter car model ([24, 13, 4]). We opt for the approximation since in real applications, the quarter car model has too many parameters compared to the expected uncertainty ([2, 13]).

We consider two types of boundary and initial condition sets for solving the equation of motion:

Model I and **Model II**. In **Model I** we consider equation (1) for the elastic beam taking it to be finite of length L with its ends freely hinged at $x = 0$ and at $x = L$. In **Model II** we consider equation (1) for the elastic beam taking it to be semiinfinite, with its end freely hinged at $x = 0$. In both cases the beam is initially at rest.

The *observation* is given by the measurement equation

(A) *Pointwise displacement sensor measurement* of $y(x^*, t)$, $t \in [0, \tau]$

$$z(t) = y(x^*, t) + \xi(t). \quad (5)$$

(B) *Pointwise acceleration sensor measurement* of $\ddot{y}(x^*, t)$, $t \in [0, \tau]$

$$z(t) = \frac{\partial^2 y(x^*, t)}{\partial t^2} + \xi(t) = \ddot{y}(x^*, t) + \xi(t). \quad (6)$$

Throughout the text y' denotes the spatial derivative $\partial y / \partial x$ in x and \dot{y} – the time derivative $\frac{\partial y}{\partial t}$ in t .

In (5) and (6), x^* is the point of measurement and $\xi(t)$ is the *measurement noise*, with $\xi(t)$ white noise with variance σ_ξ^2 (**White Noise Model**) [11, 14] or $\xi(t) = \eta(t) + u(t)$, $|u(t)| \leq \mu$, $\mu > 0$, and $\eta(t)$ white noise with variance σ_η^2 (**Bounded Noise Model**). White noise arises in applications due to electrical and transducer noise in typical sensors used for measurements [17]. Bounded noise arises due to drift observed in some sensor modalities. Typically, we also observe white noise together with the bounded noise.

In general, continuous time measurements are not available. But we sample at a high sampling rate, therefore the performance loss due to discretization is small. Also, we allow measurements to be made at several points along the highway, at x_1, \dots, x_N . The vector of observed functions is denoted by $\mathbf{z}(t)$.

Based on this model we identify three problems to be solved:

Problem 1[Force estimation] Estimate the value F on the basis of the available measurement $\mathbf{z}(t)$, $t \in [0, \tau]$. The parameters $EI, \gamma, \kappa, \beta$, in (1) are all taken as known.

Problem 2[Class detection] Suppose there are m nonintersecting intervals $\mathcal{F}_k \subset \mathbb{R}_+$:

$$\{\mathcal{F}_j \cap \mathcal{F}_k \mid j, k = 1, \dots, m; k \neq j\} = \emptyset.$$

On the basis of measurements $z(t)$, $t \in [0, \tau]$ identify to which interval \mathcal{F}_k does F belong.

Problem 3[Calibration] Given available measurements $\mathbf{z}(t)$ and an input with known dynamic force (F, ω_0) , estimate the parameters of the road model.

Observe that these problems deal with the identification of a finite number (F) through measurement of an infinite-dimensional process [17]. Also notice that the bounded noise model is more naturally related to **Problem 2** and the white noise model is better related to **Problem 1**. In this paper we focus on **Problems 1** and **2**. **Problem 3** will be addressed separately.

3 System analysis

In this section we explore the behavior of the system given in equation (1). First an analytic solution of the response of the system is computed under the assumption the beam is finite. Next an extension for the semi-infinite beam is presented, and the solution can be reduced to a particular setting of the finite beam solution. We also consider an analytic approximation to the complete solution.

[15], [25] and [3] and propose approximations of the beam response to moving loads. These approximations are different, in the sense that no guarantees on the error size of the approximation are computed, as well as the applied loads have different characteristics. Furthermore, the modulated moving characterization of the system response is not as clearly identifiable in some of these approximations. In some sense, the work in this section complements and extends previous approximation methodologies.

[4] also proposes a numerical approximation methodology to compute pavement responses, based on a state-space model [21]. The main issue of this approach for our purposes is that computing the numerical responses in real-time is much more computationally intensive than the formulas derived in this section.

3.1 Finite beam

Let us now consider equation (1) for the elastic beam taking it to be *of finite length* L , with both ends freely hinged at $x = 0$ and $x = L$ [22]. Then we have

$$y(0, t) = y(L, 0) = 0, \quad y''(0, t) = y''(L, 0) = 0, \quad t \geq 0. \quad (7)$$

We assume the beam to be originally at rest, in its equilibrium position:

$$y(x, 0) = 0, \quad \dot{y}(x, 0) = 0, \quad x \geq 0. \quad (8)$$

Therefore, the motion of the beam will arise only due to the external force $F(x, t)$. For the moving excitation, we can then show:

Theorem 3.1. *Consider the system in equation (1) with the boundary conditions (7) and (8). The response of the system excited by $F(x, t) = F \cos(\omega_0 t) \times \delta(x - Vt)$ is:*

(a) *The exact solution is given by:*

$$y(x, t) = \frac{2}{L} \sum_{m=0}^{\infty} Y_m(t) \sin\left(\frac{\pi m x}{L}\right), \quad (9)$$

where $Y_m(t)$ is given in equation (10), and is composed by two parts $Y_{tr,m}(t)$, the transient natural beam response, and $Y_{ss,m}(t)$, the "steady-state" component, corresponding to the response

of the beam to the excitation:

$$\begin{aligned}
Y_m(t) &= Y_{tr,m}(t) + Y_{ss,m}(t), \tag{10} \\
Y_{ss,m}(t) &= \frac{F_0}{2} \{ |F_{a,m}| \sin(\omega_{a,m}t + \angle|F_{a,m}|) + |F_{b,m}| \sin(\omega_{b,m}t + \angle|F_{b,m}|) \}, \\
Y_{tr,m}(t) &= \frac{F_0}{2\Omega_m} e^{-kt} (|C_{a,m}| \sin(\Omega_m t + \angle C_{a,m}) + |C_{b,m}| \sin(\Omega_m t + \angle C_{b,m})), \\
F_0 &= \frac{F}{\gamma}, \quad k = \frac{\kappa}{\gamma}, \quad \omega_m^2 = (\alpha(\pi m/L)^4 + \beta)/\gamma, \quad \Omega_m^2 = \omega_m^2 - k^2 \\
\omega_{a,m} &= \frac{\pi m}{L}V + \omega_0, \quad \omega_{b,m} = \frac{\pi m}{L}V - \omega_0, \\
C_{a,m} &= \frac{1}{k^2 - 2k\Omega_m i - \Omega_m^2 + \omega_{a,m}^2}, \\
C_{b,m} &= \frac{1}{k^2 - 2k\Omega_m i - \Omega_m^2 + \omega_{b,m}^2}, \\
F(s, m) &= s^2 + 2ks + \omega_m^2, \\
F_{a,m} &= F(i\omega_{a,m}, m)^{-1}, \\
F_{b,m} &= F(i\omega_{b,m}, m)^{-1} = F^*(i\omega_{a,m}, -m)^{-1}.
\end{aligned}$$

(b) We have:

$$\lim_{L \rightarrow \infty} y(x, t) = F_0 \text{Re}[\psi^*(Vt - x)e^{j\omega_0 t}] + O(e^{-kt}),$$

where

$$\begin{aligned}
\psi^*(t) &= \frac{1}{2\pi i} \int_{-\infty}^{\infty} \Omega(s)^{-1} e^{st} ds, \\
\Omega(s) &= \alpha/\gamma s^4 + V^2 s^2 + (2\omega_0 V i + 2kV)s + (\beta/\gamma - \omega_0^2 + 2k\omega_0 i). \tag{11}
\end{aligned}$$

(c) The response of system (1) to the fixed excitation $F(x, t) = F\delta(t - t_0)\delta(x - x_0)$ is given by:

$$\begin{aligned}
\tilde{Y}_m(t) &= F_0 \Omega_m^{-1} e^{-kt} \sin(\Omega_m t) u(t), \\
y(x, t) &= \frac{2}{L} \sum_{m=0}^{\infty} \tilde{Y}_m(t - t_0) \cos\left(\frac{\pi m(x - x_0)}{L}\right) - \frac{2}{L} \sum_{m=0}^{\infty} \tilde{Y}_m(t - t_0) \cos\left(\frac{\pi m(x + x_0)}{L}\right),
\end{aligned}$$

where the Heaveside function $u(t)$ is defined as $u(t) = 1$ for $t \geq 0$ and $u(t) = 0$ for $t < 0$.

The solution in Theorem 3.1 does not solve for the truck forcing term (equation (2)), but since the PDE is linear, the result is easily extended.

Corollary 1. *Let*

$$h(x, t|\omega_0, V) = \frac{1}{\gamma} \text{Re}[\psi^*(Vt - x)e^{j\omega_0 t}], \tag{12}$$

where ψ^* is computed according to equation (48) with parameters ω_0 and V . Then the response of system (1) to the truck forcing term (equation (2)) is given by

$$\lim_{L \rightarrow \infty} y(x, t) = F(h(x, t|0, V) + h(x, t|\omega_0, V)) + O(e^{-kt}) \quad (13)$$

The qualitative behavior of the system can be explored using Theorem 3.1(c). The closed form solution for the displacement $y(x, t)$ can be obtained by computing the inverse Laplace transform [21] of $\Omega(s)^{-1}$ as shown. Inverting Laplace transforms requires the specification of the region of convergence (ROC) of the integral [21]. Since the system we are dealing is a physical system, the solution obtained from the inversion computation should be a solution with bounded energy.

The standard inversion procedure starts by computing the roots of the rational transfer function to be inverted. In the present case this corresponds to finding the values λ_i such that $\Omega(\lambda_i) = 0$, which amounts to solving for the roots of a fourth order polynomial. Then we can use the partial fraction expansion, and assuming no repeated roots, to obtain the decomposition:

$$\Omega(s)^{-1} = \sum_{i=1}^4 \frac{A_i}{s - \lambda_i},$$

where A_i are the partial fraction expansion coefficients. Using the bounded energy condition as the region of convergence rule, the inverse Laplace transform states:

$$\frac{1}{2\pi} \int_{-\infty}^{\infty} \frac{A_i}{s - \lambda_i} e^{st} ds = \begin{cases} A_i e^{\lambda_i t} u(t) & \text{Re}[\lambda_i] \leq 0 \\ -A_i e^{\lambda_i t} u(-t) & \text{Re}[\lambda_i] > 0 \end{cases}.$$

Since the coefficient that follows s^3 in the polynomial $\Omega(s)$ is zero, we have that $\lambda_1 + \lambda_2 + \lambda_3 + \lambda_4 = 0$, which implies that either $\text{Re}[\lambda_i] = 0$ for all the roots, or else, there are roots with $\text{Re}[\lambda_i] > 0$ and with $\text{Re}[\lambda_i] < 0$. The beam is damped, therefore not all roots can be $\text{Re}[\lambda_i] = 0$. Without loss of generality, let us assume that $\text{Re}[\lambda_1] > 0$, $\text{Re}[\lambda_2] > 0$, $\text{Re}[\lambda_3] < 0$ and $\text{Re}[\lambda_4] < 0$. Then, the function $\psi^*(t)$ in Theorem 3.1(c) can be computed as

$$\psi^*(t) = -A_1 e^{\lambda_1 t} u(-t) - A_2 e^{\lambda_2 t} u(-t) + A_3 e^{\lambda_3 t} u(t) + A_4 e^{\lambda_4 t} u(t).$$

The beam deflection response is essentially a traveling wave shaped by $\psi^*(t)$. The shape of ψ^* implies that there is a decaying behavior for large $t > 0$ and for small $t < 0$. Moreover, the time t^* at which the truck goes over the location x is $t^* = x/V$. At this time, the value of the wave shape is $\psi^*(0)$. This also implies that at location x the beam experiences some displacement even before the truck arrives at that location, since $\psi^*(t) \neq 0$ for $t < 0$. This displacement is caused by the sum of the excitations just prior to the truck arriving at that location. The whole response is modulated by the truck's suspension system frequency. This accurately captures the important phenomena observed in the more complex quarter car model [2, 13].

A better comprehension of the behavior of the roots can be gained by looking at the system response for large truck speeds. Consider the transform $s' = i\omega_0 + V s$. Then, the polynomial can

be written as:

$$\begin{aligned}\Omega(s') &= s'^2 + 2k s' + \frac{\beta}{\gamma} + \frac{\alpha}{\gamma V^4} (s' - i\omega_0)^4 \\ &\approx s'^2 + 2k s' + \frac{\beta}{\gamma}\end{aligned}$$

Thus the roots of the original $\Omega(s)$ at high speed are given by

$$\lambda_{1,2} = \frac{-k \pm \sqrt{\beta/\gamma - k^2}i - \omega_0 i}{V}.$$

The displacement can be computed as:

$$y(x, t) \approx \frac{F}{\gamma V \sqrt{\beta/\gamma - k^2}} e^{-k(t - \frac{x}{V})} \sin\left(\sqrt{\beta/\gamma - k^2} \left(t - \frac{x}{V}\right)\right) \cos\left(\frac{\omega_0 x}{V}\right). \quad (14)$$

The exponential decay of the solution is at a rate $-k$ (notice the normalization by V) independent of speed, and the fundamental frequencies of the system is $\sqrt{\beta/\gamma - k^2}$. At high speeds, the suspension system modulation frequency ω_0 only affects the amplitude of the response spatially.

To conclude the discussion, the solution for a fixed excitation (Theorem 3.1 (d)) can be related to the moving excitation solution. Let $t_0 = x/V$ and $x_0 = Vt$ in the fixed excitation. This is similar to having an unmodulated moving impulse without iterating through the physical system. Then:

$$y(x, t) = \frac{2}{L} \sum_{m=0}^{\infty} \tilde{Y}_m(Vt - x) \cos\left(\frac{\pi m(Vt - x)}{L}\right) - \frac{2}{L} \sum_{m=0}^{\infty} \tilde{Y}_m(Vt - x) \cos\left(\frac{\pi m(x + Vt)}{L}\right),$$

which is the solution for the moving excitation when $\omega_0 = 0$.

3.2 Semi-infinite beam

For completeness, we consider system (1) for the elastic beam taking it to be semiinfinite, with its end freely hinged at $x = 0$ [7, 22]. The important observation is that the obtained solution is equivalent to the solution obtained for a finite beam of length L by letting $L \rightarrow \infty$, confirming the validity of our approximation. The computation of the current solution, though, relies on a continuous Fourier transform decomposition [7, 22].

Since the end is freely hinged, the boundary conditions are then given by

$$y(0, t) = 0, \quad y''(0, t) = 0, \quad t \geq 0, \quad (15)$$

We assume the beam to be originally at rest, in its equilibrium position:

$$y(x, 0) = 0, \quad \dot{y}(x, 0) = 0, \quad x \geq 0. \quad (16)$$

Furthermore, also presume that the derivatives $y^{(k)}(x, t)$, $k = 1, \dots, 3$, vanish at $x = \infty$, which is equivalent to the limit of the condition we used at $x = L$ for a finite beam. We can then show

Theorem 3.2. *The exact solution for the moving excitation hinged semi-infinite beam problem is given by:*

$$y(x, t) = (2/\pi)^{\frac{1}{2}} \int_0^{\infty} Y_{\xi}(t) \sin(\xi x) d\xi, \quad (17)$$

where

$$Y_{\xi}(t) = Y_{\frac{\xi L}{\pi}}(t), \quad (18)$$

and Y_m is given in Equation (10).

4 Estimating the load

Problem 1 concerns the estimation of the weight under the **White Noise Model**, given that the parameters of the highway are known [3]. The input to the highway system is a truck, whose corresponding forcing model is given by

$$F(x, t) = F(1 + \cos(\omega_0[t - t_0] + \phi)) \times \delta(x - V[t - t_0]), \quad (19)$$

where we have included the phase term ϕ to account for the uncertainty in the initial conditions of the suspension system for the truck and t_0 to account for the unknown initial starting time of the truck.

We assume two types of situations. In the coherent estimation problem, we assume that the truck parameters t_0, ϕ, ω_0 , and V are known, and we have to estimate the value of F . In a certain sense, this is the best possible situation, since the whole parametrization of the problem is known.

The conditions are progressively relaxed, assuming first that t_0 is unknown, both ϕ and t_0 are unknown, and finally t_0, ω_0 and ϕ are unknown. We assume that the speed V can be measured, but at the end of the section we study the sensitivity of our problem towards this parameter. The problems with less information are categorized as non-coherent estimation problems, and as we will see there are considerable noise tradeoffs in such scenarios. One of the issues with non-coherent estimation is that the identifiability of the force F depends on the information set. Denote the information set as \mathcal{I} , such as in $\mathcal{I} = [V, \omega_0, \phi]$.

The first important observation is about the role of the measurement equation. For the methods presented here, the fact that displacement is being measured (equation (5)) or acceleration is being measured (equation (6)) does not change the methodology. The error rates of the proposed methods though could be different since they depend on the amount of energy measured by the transducer relative to the amount of noise. To normalize our error computations, we define the signal-to-noise

ration (SNR) of the measurement system as [14, 17]:

$$\begin{aligned} P_\xi &= \mathbb{E} \left[\int_0^\tau \xi(t)^2 dt \right], \quad P_s = \mathbb{E} \left[\int_0^\tau z(t)^2 dt \right], \\ \text{SNR} &= \frac{P_s - P_\xi}{P_\xi}, \end{aligned} \quad (20)$$

which is a surrogate measure of the relative amount of information being captured by the sensor. We assume without loss of generality, that the measurement is displacement. Also, for the remainder of the section, denote by $h(t, x|V, \omega_0, \phi)$, the response to the forcing equation (19):

$$h(x, t|\omega_0, V, \phi, t_0) = \frac{1}{\gamma} \text{Re}[\psi_1^*(V[t - t_0] - x)e^{j(\omega_0(t-t_0)+\phi)}] + \frac{1}{\gamma} \text{Re}[\psi_0^*(V[t - t_0] - x)e^{j\phi}], \quad (21)$$

where ψ_1^* is computed according to equation (48) with parameters ω_0 and V , and ψ_0^* computed with parameters $\omega_0 = 0$ and V . This result can be demonstrated with a minor modification in the proof of Theorem 3.1.

Furthermore, we allow the observation to be a scalar function $z(t)$, at a single point in space x^* , or more generally, $z_i(t)$, at points in space x_i^* for $i = 1, \dots, I$, implying measurements with I sensors. Procedures for different information sets are shown in Theorem 4.1. Notice that as more parameters become unknown, the complexity of the procedure increases.

Theorem 4.1. *Given the complete information set $\mathcal{I}_0 = [V, \omega_0, \phi, t_0]$, the optimal mean square estimate of the parameter F is*

(a) *For a single observation at x^**

$$\hat{F} = \int_0^\infty \frac{z(t)h(t, x^*|\omega_0, V, \phi, t_0)}{\|h(t, x^*|\omega_0, V, \phi, t_0)\|^2} dt, \quad (22)$$

and the Mean Square Error (MSE) is given by

$$\mathbb{E}[(\hat{F} - F)^2] = \frac{\sigma^2}{\|h(t, x^*|\omega_0, V, \phi, t_0)\|^2}, \quad (23)$$

$$= \frac{1}{\text{SNR}(x^*)} \quad (24)$$

(b) *For multiple observations x_i^* , $i = 1, \dots, I$:*

$$\hat{F} = \frac{\sum_{i=1}^I \int_0^\infty z_i(t)h(t, x_i^*|\omega_0, V, \phi, t_0) dt}{\sum_{i=1}^I \|h(t, x_i^*|\omega_0, V, \phi, t_0)\|^2}, \quad (25)$$

The MSE is

$$\mathbb{E}[(\hat{F} - F)^2] = \sum_{i=1}^I \frac{1}{\text{SNR}(x_i^*)}, \quad (26)$$

Given the information set $\mathcal{I}_1 = [V, \omega_0, \phi]$, the energy estimate of the parameter F is

(c) For a single observation at x^*

$$\hat{F} = \left[\frac{\int_0^\tau z(t)^2 dt}{\|h(t, x^* | \omega_0, V, \phi, 0)\|_\tau^2} \right]^{\frac{1}{2}}, \quad (27)$$

(d) For multiple observations x_i^* , $i = 1, \dots, I$:

$$\hat{F} = \frac{\sum_{i=1}^I \int_0^\infty z_i(t)^2 dt}{\sum_{i=1}^I \|h(t, x_i^* | \omega_0, V, \phi, 0)\|_\tau^2}, \quad (28)$$

Given the information set \mathcal{I}_i , where \mathcal{I}_0 represents the complete information set, denote by $\mathcal{I} = \mathcal{I}_0 - \mathcal{I}_i$ the set of unknown parameters. Then

(e) For a single observation at x^* , the least-squares estimator is

$$\hat{\mathcal{I}} = \arg \max_{\mathcal{I}} \frac{\left(\int_0^\infty z(t) h(t, x^* | \omega_0, V, \phi, t_0) dt \right)^2}{\|h(t, x^* | \omega_0, V, \phi, t_0)\|^2} \quad (29)$$

$$\hat{F} = \frac{\left| \int_0^\infty z(t) h(t, x^* | \mathcal{I}_i \cup \hat{\mathcal{I}}) dt \right|}{\|h(t, x^* | \mathcal{I}_i \cup \hat{\mathcal{I}})\|^2} \quad (30)$$

(f) For multiple observations x_i^* , $i = 1, \dots, I$:

$$\hat{\mathcal{I}} = \arg \max_{\mathcal{I}} \frac{\left(\sum_{i=1}^I \int_0^\infty z(t) h(t, x_i^* | \omega_0, V, \phi, t_0) dt \right)^2}{\sum_{i=1}^I \|h(t, x_i^* | \omega_0, V, \phi, t_0)\|^2} \quad (31)$$

$$\hat{F} = \frac{\left| \sum_{i=1}^I \int_0^\infty z(t) h(t, x_i^* | \mathcal{I}_i \cup \hat{\mathcal{I}}) dt \right|}{\sum_{i=1}^I \|h(t, x_i^* | \mathcal{I}_i \cup \hat{\mathcal{I}})\|^2} \quad (32)$$

The first insight that Theorem 4.1 gives is that in the full information case, the optimal estimator guarantees that the mean squared error decreases as $O(1/I)$, where I is the number of sensors. So in theory increased precision in the force estimation can be obtained by adding additional sensors to the system. In practice the limits are the uncertainties about the speed over a longer stretch of pavement might limit this performance.

The second observation is that as the information set becomes smaller, the complexity of the optimization needed to be carried out increases. For example, for the information set $\mathcal{I}_4 = \{V\}$, an optimization over the three remaining parameters ω_0 , t_0 and ϕ needs to be carried out. The optimization itself is not convex, but the domain is bounded in ω_0 and ϕ . This fact can be used to devise a more efficient optimization methodology.

To conclude the section, we note that the result for the **Bounded Noise Model** is identical to the **White Noise Model**.

5 System design

In this section we address some important considerations when building a practical system for axel dynamic force computation. The first important consideration is the spatial placement of the acceleration sensors, which can result in improved estimation of the force. The next important consideration is how to implement a computation system for the axel force, based on the methodology suggested in section 4. Some considerations about the most efficient approaches to compute the optimization should be made. Both issues are addressed in this section.

5.1 Sensor placement and design

Natural constraints on the placement of the sensor arise from observing the system response function to the moving load (Theorem 3.1(c)). The constraints are driven by observability requirements of the output of the system. The first important natural constraint arises from the observation that taking samples of sensors at different sensors at locations x_i , at times $t_i = x_i/V + \delta$, for some constant δ , we obtain the response function

$$y(t_i, x_i) = F_0 \operatorname{Re}[\psi^*(\delta)] \cos(\omega_0/V x_i + \omega_0 \delta) + F_0 \operatorname{Im}[\psi^*(\delta)] \sin(\omega_0/V x_i + \omega_0 \delta) + O(e^{-k(\frac{x_i}{V} + \delta)}).$$

The Nyquist condition [20] implies that the sampling rate has to be less than twice the highest frequency of the signal, for uniformly sampled spatial signals. If we assume that sensors are placed uniformly according to $x_i = i \Delta x$, and the bandwidth of $y(t_i, x_i)$ is $\Delta \omega_0$, the condition becomes

$$\frac{2\pi}{\Delta x} \geq 2\Delta \omega_0.$$

The truck suspension system parameter ω_0 is in the range $\omega_0 \in 2\pi[1, 3]$, therefore $\Delta \omega_0 = 2\pi(3-1)/V$ for the signal of interest, and we can conclude the following requirement on the sensor placement:

$$\Delta x \leq \frac{V}{4} \text{ (meters)}.$$

Interestingly, the minimum speed of the truck in the system is the limitation on how close sensors must be. If we assume that the minimum speed is 30 mph, the sensors must be at most 3.35 meters apart for observability of the measurement.

Similarly, the fundamental frequencies in the function ψ^* play a role as well. For each root λ_i of the system function $\Omega(s)$ in (Theorem 3.1(c)), the Nyquist criterion applies, therefore

$$\Delta x \leq \frac{2\pi}{2 \max_i \lambda_i} \text{ (meters)}.$$

For high speeds V of the truck, Equation 14 shows that both conditions can be simplified to the condition

$$\Delta x \leq \frac{2\pi V}{2(\Delta \omega_0 + \sqrt{\beta/\gamma - k^2})} \text{ (meters)}.$$

5.2 Distributed data computation

The optimization in Equation (29) is complex when the information set is small. The optimization is not convex, but is in a bounded domain, which facilitates a simple approach. We consider here the smallest information set, $\mathcal{I} = \{V\}$. The procedure can be adjusted for other information sets in a straightforward manner.

The parameter t_0 is a time shift parameter, and can be optimized separately. One choice is to compute a cross correlation [14, 17], which consists in calculating the objective function for a series of values of t_0 in some window of interest $[T_1, T_2]$ where the energy of the signal $z(t)^*$ is greater than the noise floor. Another choice is to compute Fourier transforms of both $z(t)^*$ and the normalized signal

$$\tilde{h}(t, x_i^*) = \frac{h(t, x_i^* | \omega_0, V, \phi, 0)}{\sqrt{\sum_{i=1}^I \|h(t, x_i^* | \omega_0, V, \phi, 0)\|^2}} \quad (33)$$

and use Parseval's relation to obtain:

$$\hat{\mathcal{I}} = \arg \max_{\mathcal{I} - \{t_0\}} \left(\sum_{i=1}^I \int_{-\infty}^{\infty} Z(\omega) \tilde{H}(\omega, x_i^* | \omega_0, V, \phi, 0)^* d\omega \right)^2$$

$$\hat{F} = \left| \sum_{i=1}^I \int_{-\infty}^{\infty} Z(\omega) \tilde{H}(\omega, x_i^* | \omega_0, V, \phi, 0)^* d\omega \right| / \sqrt{\int_{-\infty}^{\infty} |H(\omega, x_i^* | \omega_0, V, \phi, 0)|^2 d\omega}.$$

6 Simulation

In this section we examine the behavior of the pavement-truck system and the quality of the proposed weight estimation schemes. First we compute the responses of the system to a variety of changes in the parameters representing the truck such as its speed V and suspension frequency ω_0 . We use the following parameter values for the pavement [2]¹:

$$EI = 1.38 \times 10^6 Nm^2; \beta = 170 \times 10^6 N/m^2; \gamma = 353 \times 10^3 kg/m; \kappa = 10^6 Ns/m^2, \quad (34)$$

where we have assumed $M = 10^6$; $g = 10m/s^2$. We take the axel weight of the truck to be 5000 Kg, therefore $F_0 = 50000N$. Whenever unspecified, we take the suspension system fundamental frequency to be $\omega_0 = 1.23Hz$.

The observed measurements are acceleration measurements and follow the noise **Model I**. The measurement noise is assumed zero mean white noise with standard deviation $\sigma_w = 120 \mu g$ (micro-g's), which is the expected noise power for a measurement system based on MEMS accelerometers.

In the second part of the section we compute error distributions for the proposed weight estimation methodology. As we will see, the proposed method is quite robust to noise in the acceleration measurements.

¹In the book these parameters are: $EI = 1.38MNm^2; \beta = 170MN/m^2; \gamma = 353Mg/m; \kappa = 1MNs/m^2$.

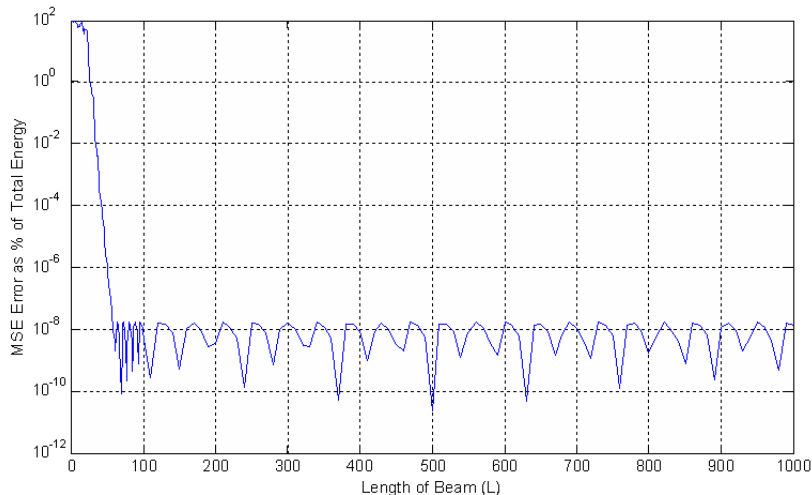


Figure 2: Relative Mean Squared Error (%) between ground truth displacement and asymptotic approximation at $L/2$ for $V = 10$ m/s ($y(L/2, t)$).

6.1 Pavement response

The main difficulty in simulating the distributed system (Equation (1)) is its stiffness with respect to parameters in Equation (34) [4]. Stiffness means that small variations on the forcing function $F(x, t)$ cause large variations in the output $y(x, t)$. This is the case for any pavement model, given that the material structure itself is not very flexible and therefore the system will exhibit a stiff response [13].

The pavement response to a moving load can be computed exactly by using Theorem 3.1(Eq. (9)). The solution is a convergent infinite summation. The summation cannot be computed exactly, but can be approximated by truncating at a predetermined number of terms. Lemma 7.1 shows that the truncation has exponential decay so the ignored part will only contribute a finite amount to the error. Unfortunately, such solution does not give much insight on the behavior of the system. Furthermore, for the parameters in Equation (34), the pavement exhibits a very stiff behavior, and the number of terms required is quite large. For the reported parameters, we observed that at least 5,000 elements were required before the norm of the additional terms being added is a small fraction of the sum at that point.

An alternative approach is to compute a direct numerical solution to the original PDE (Equation (1)). A Finite Element Method is indicated for this problem. The publicly available state-of-the-art FlexPDE solver can be used. Due to the high degree of stiffness of the PDE, the solver has difficulties finding acceptable numerical approximations to the response since it has to handle very poorly conditioned matrix inversions. In our experiments, the numerical approximation resulted in solutions qualitatively correct but with severe kinks, which are not physically valid.

The closed form approximation in Theorem 3.1(b) is easy to compute. The solution is exact as the length $L \rightarrow \infty$. It is important then to evaluate the quality of the approximation for finite

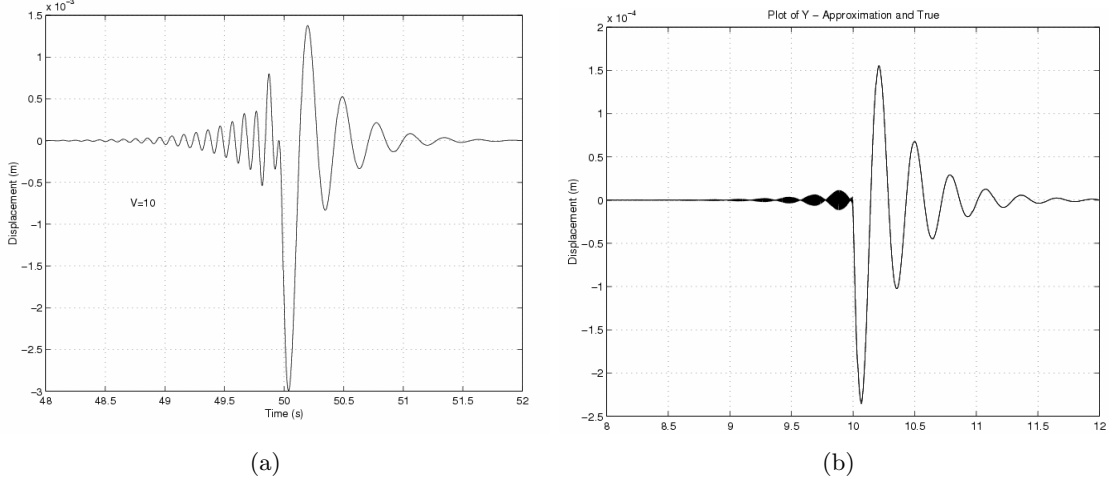


Figure 3: (a) Displacement at $x = 500$ m, for $L = 1000$ m, $V = 10$ m/s and $\omega_0/2\pi = 1.23$ Hz. Fundamental frequencies (amplitudes) for the signal before $t = 50$ s are 4.7 Hz (14.2) and 9.8 Hz (2.8). After $t = 50$ s they are 3.7 Hz (13.8) and 3.5 Hz (3.1). (b) Displacement at $x = 500$ m, for $L = 1000$ m, $V = 50$ m/s and $\omega_0/2\pi = 1.23$ Hz.

values of L . As the gold standard we choose the truncated solution based on Theorem 3.1(b), with a large number of coefficients, $N = 10,000$, where it is observed computationally that the summation has converged to a degree. The relative mean squared error is used for comparison purposes:

$$\text{Err}(r(t), y(t)) = \frac{\int_0^\tau (r(t) - y(t))^2 dt}{\int_0^\tau r(t)^2 dt} \quad (35)$$

Figure 2 shows the relative mean squared difference between the ground truth solution and the asymptotic approximation, in percentages. A fixed position $x = L/2$ was chosen. Of course the solution is accurate away from the boundaries, and in our highway problem we are only interested in the behavior away from the virtual boundaries as well. Notice that very quickly the error becomes negligible. It is safe to say that for $L > 50$ m, we have an accurate solution for the given parameters choice.

Simulation results

Figure 6.1 shows the displacement $y(x, t)$ at $x = 500$ m. The peak of the response happens at $t = 50$ s as expected. Furthermore, even before the truck arrives at $x = 500$ m, there is a response signal being generated. This is a typical characteristic of a distributed parameter wave system. We also computed the signal frequencies before and after the arrival of the truck at $x = 500$ m. A single frequency before and a single frequency after are responsible for most of the response. As we saw in the theoretical section, the frequencies before the arrival of the truck at $x = 500$ m consist of the imaginary parts of the anti-causal poles of the response transfer function and the frequencies after correspond to the imaginary part of the causal poles.

One interesting feature is that the signal after the truck arrival vibrates at a smaller frequency

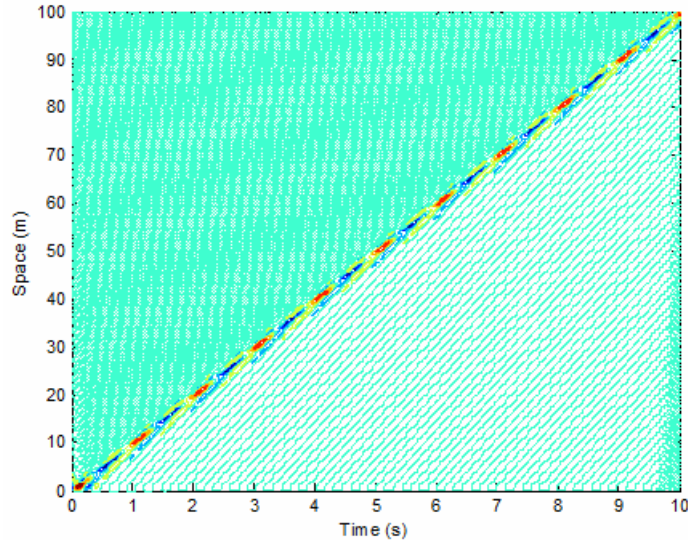


Figure 4: Contour plot of displacement $y(x, t)$, for $L = 1000$ m, $V = 10$ m/s and $\omega_0/2\pi = 1.23$ Hz.

than the signal before. In physical terms it can be understood as a doppler type phenomenon, but the waves being propagated are vibrations and the propagation medium is the pavement.

Figure 4 shows the wave behavior of the displacement response. The response is approximately localized in space and time, i.e., at any given fixed measurement point, there is a window of useful data. Furthermore the figure also shows more clearly the effects of modulating the typical response. In summary, the displacement response at any point in space is an appropriately shifted and modulated version of the response at any other point, with fix modulation frequency but variable phase.

In Section 3 we computed the asymptotic pole locations as the velocity of the truck become high. The fourth order polynomial reduced to a second order polynomial with causal complex roots. That is, the response of the pavement before the truck arrives at the measurement location is negligible compared to the response after. Figure shows the response with the truck at a higher speed, confirming this asymptotic viewpoint.

Figure 5 shows the variation of the magnitudes of the real and imaginary parts of the poles of the response with respect to the speed. As the speed becomes higher, we see that a pair of the imaginary frequencies tend to a small value. Furthermore, the remaining pair increases linearly with speed and becomes approximately conjugate. This behavior also means that the expansion coefficients for the small value imaginary frequency poles become small, as they are directly proportional to the product of the magnitude of the remaining poles. Thus, as speed increases, the 4 pole system collapses to a two pole system approximately. This observation will be useful to calibrate the model PDE. The Figure also shows the real part of the poles, and they confirm the notion that as the speed becomes higher we end up with a pair of causal complex conjugate poles and possibly a pair of anti-causal complex conjugate poles.

Finally, Figure 6 shows the impulse response for an impulse located at $x = 500$ m. Notice that

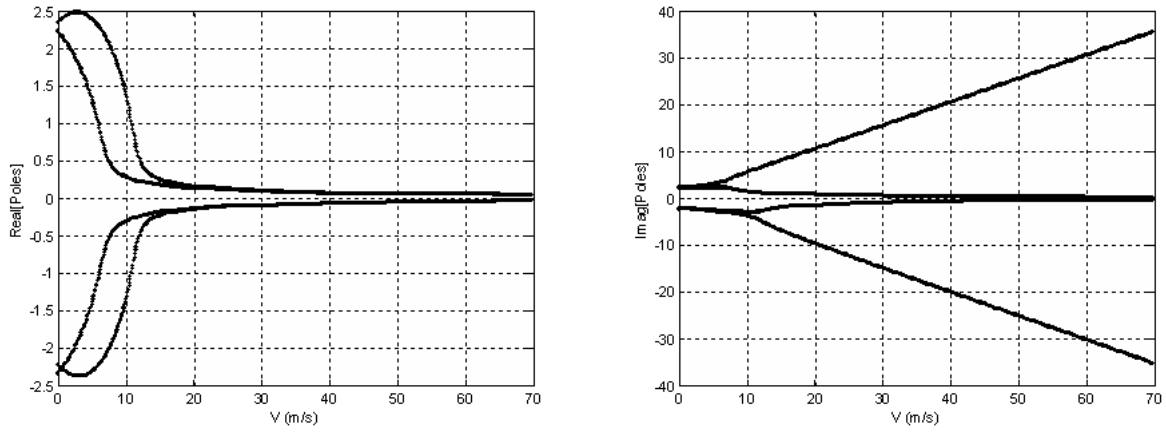


Figure 5: Real and imaginary parts of the poles of the system for $L = 1000$ m and $\omega_0/2\pi = 1.23$ Hz.

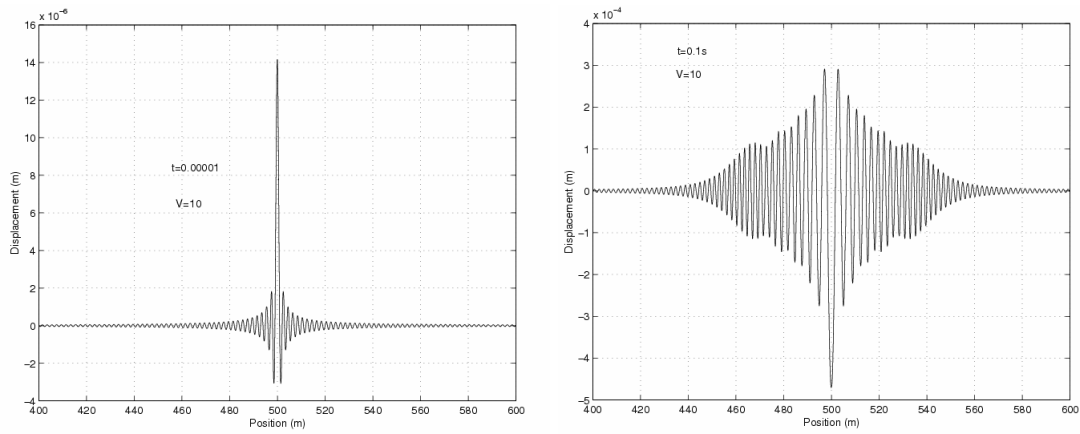


Figure 6: Displacement impulse response along the highway, for $L = 1000$ m, at (a) $t = 0.00001$ s and (b) $t = 0.1$ s.

now the oscillation is symmetric.

7 Proofs

7.1 Theorem 3.1

(a) A Fourier expansion should be use to solve the equation [22]. The basis choice is constrained by the boundary condition [7, 22]. There are four available basis $\sin \frac{\pi mx}{L}$, $\cos \frac{\pi mx}{L}$, $\sinh \frac{\pi mx}{L}$ and $\cosh \frac{\pi mx}{L}$. The four boundary conditions are used to determine the right expansion to use. Using a Fourier type expansion on the basis $\{\sin \frac{\pi mx}{L}\}$, integrating from 0 to L by parts and taking into account the boundary conditions (7) at $x = 0$ and $x = L$, we obtain the relations

$$\begin{aligned} \int_0^L y''''(x, t) \sin(\pi mx/L) dx &= -(\pi m/L)^2 \int_0^L y''(x, t) \sin(\pi mx/L) dx \\ &= (\pi m/L)^4 \int_0^L y(x, t) \sin(\pi mx/L) dx. \end{aligned} \quad (36)$$

We further proceed as follows. We multiply both sides of equation (1) by $\sin(\pi mx/L)$ and integrate them from 0 to L in x . Further on, denoting $EI = \alpha$ and dividing both parts by γ , we come to equation

$$\ddot{Y}_m + 2k\gamma^{-1}\dot{Y}_m + (\alpha(\pi m/L)^4 + \beta)\gamma^{-1}Y_m = F\gamma^{-1} \cos \omega_0 t \sin(\pi mVt/L) \quad (37)$$

with initial condition $Y_m(0) = \dot{Y}_m(0) = 0$.

Here

$$Y_m(t) = \int_0^L y(x, t) \sin(\pi mx/L) dx$$

is the *finite Fourier sine coefficient* of function $y(x, t)$. The right-hand side arrived through formula

$$\int_0^L F \cos \omega_0(t) \sin(\pi mx/L) \delta(x - Vt) dx = F \cos \omega_0 t \sin(\pi mVt/L)$$

Using the definitions for k, F_0, ω_m^2 and Ω_m^2 we come to equation

$$\ddot{Y}_m + 2k\dot{Y}_m + \omega_m^2 Y_m = F_0 \cos \omega_0 t \sin(\pi mVt/L) \quad (38)$$

with zero initial conditions for each m .

We can now solve this equation by using the following simplification:

$$\ddot{Y}_m + 2k\dot{Y}_m + \omega_m^2 Y_m = \frac{F_0}{2} \sin((\pi mV/L + \omega_0)t) + \frac{F_0}{2} \sin((\pi mV/L - \omega_0)t) \quad (39)$$

Noticing that the roots of the differential equation are $k \pm \Omega_m i$ since $\beta > \kappa$ (implying $\omega_m^2 > k$), we can write the full response to the above ODE as in Equation (10) [21].

(b) First we show that the transient part of the complete response to a moving excitation is $O(1)$ for the total transient response:

$$Y_{tr}(x, t) = \frac{2}{L} \sum_{m=0}^{\infty} Y_{tr,m}(t) \sin\left(\frac{\pi m x}{L}\right) \quad (40)$$

Lemma 7.1. $Y_{tr}(x, t) = O(e^{-kt})$, uniformly in x . Furthermore, $\lim_{L \rightarrow \infty} Y_{tr}(x, t) = O(e^{-kt})$, uniformly in x .

Proof. From the definitions:

$$\begin{aligned} |Y_{tr}(x, t)| &= \left| \frac{2}{L} \sum_{m=0}^{\infty} Y_{tr,m}(t) \sin\left(\frac{\pi m x}{L}\right) \right| \\ &\leq \frac{2}{L} \sum_{m=1}^{\infty} |Y_{tr,m}| \\ &\leq F_0 e^{-kt} \frac{2}{L} \sum_{m=1}^{\infty} \frac{1}{\Omega_m^3} \\ &\leq F_0 e^{-kt} \frac{2}{L} \sum_{m=1}^{\infty} \frac{\gamma^{\frac{3}{2}}}{\alpha^{\frac{3}{2}} \pi^6 (m/L)^6} \\ &= \frac{2F\gamma^{\frac{1}{2}}}{\alpha^{\frac{3}{2}} \pi^6} e^{-kt} K(L), \end{aligned} \quad (41)$$

where

$$K(L) = \frac{1}{L} \sum_{m=1}^{\infty} \frac{1}{(m/L)^6}.$$

For each finite L it is clear that $K(L) < \infty$. Moreover:

$$\begin{aligned} \lim_{L \rightarrow \infty} K(L) &< \int_1^{\infty} \frac{1}{s^6} ds \\ &= 1/7 \end{aligned}$$

□

We can now consider $Y_{ss,m}(t)$. Isolating the modulation of the forcing term:

$$\begin{aligned} Y_{ss,m}(t) &= \frac{F_0}{2} \left\{ |F_{a,m}| \sin\left(\frac{\pi m V}{L} t + \angle|F_{a,m}|\right) + |F_{b,m}| \sin\left(\frac{\pi m V}{L} t + \angle|F_{b,m}|\right) \right\} \cos(\omega_0 t) + \\ &+ \frac{F_0}{2} \left\{ |F_{a,m}| \cos\left(\frac{\pi m V}{L} t + \angle|F_{a,m}|\right) - |F_{b,m}| \cos\left(\frac{\pi m V}{L} t + \angle|F_{b,m}|\right) \right\} \sin(\omega_0 t) \end{aligned} \quad (42)$$

We can now incorporate the sine term in Equation (9), using sine and cosine identities and moving

constants around:

$$f(r) = \frac{1}{2L} \sum_{m=0}^{\infty} |F_{a,m}| \cos\left(\frac{\pi m}{L}r + \angle|F_{a,m}|\right) + |F_{b,m}| \cos\left(\frac{\pi m}{L}r + \angle|F_{b,m}|\right) \quad (43)$$

$$g(r) = \frac{1}{2L} \sum_{m=0}^{\infty} |F_{a,m}| \sin\left(\frac{\pi m}{L}r + \angle|F_{a,m}|\right) - |F_{b,m}| \sin\left(\frac{\pi m}{L}r + \angle|F_{b,m}|\right) \quad (44)$$

$$y(x, t) = F_0\{(f(Vt - x) - f(Vt + x)) \cos(\omega_0 t) + (g(Vt + x) - g(Vt - x)) \sin(\omega_0 t)\} \quad (45)$$

Now we can compute the following quantity:

$$f^*(r) = \lim_{L \rightarrow \infty} \frac{1}{2L} \sum_{m=0}^{\infty} |F_{a,m}| \cos\left(\frac{\pi m}{L}r + \angle|F_{a,m}|\right) + |F_{b,m}| \cos\left(\frac{\pi m}{L}r + \angle|F_{b,m}|\right) \quad (46)$$

Defining the constants

$$\begin{aligned} \omega_{a,\xi} &= \pi\xi V + \omega_0, & \omega_{b,\xi} &= \pi\xi V - \omega_0, \\ \omega_{\xi}^2 &= (\alpha(\pi\xi)^4 + \beta)/\gamma, & \hat{\omega}_{a,\xi} &= \xi V + \omega_0, \\ F(s, \xi) &= s^2 + 2ks + \omega_{\xi}^2 \\ F_{a,\xi} &= F(i\omega_{a,\xi}, \xi)^{-1} \\ F_{b,\xi} &= F(i\omega_{b,\xi}, \xi)^{-1} = F^*(i\omega_{a,\xi}, -\xi)^{-1}, \end{aligned}$$

we can obtain

$$\begin{aligned} f^*(r) &= \frac{1}{2} \int_0^{\infty} \{|F_{a,\xi}| \cos(\pi\xi r + \angle|F_{a,\xi}|) + |F_{b,\xi}| \cos(\pi\xi r + \angle|F_{b,\xi}|)\} d\xi \\ &= \frac{1}{2\pi} \int_{-\infty}^{\infty} |F(i\hat{\omega}_{a,\xi}, \xi)^{-1}| \cos(\xi r + \angle F(i\hat{\omega}_{a,\xi}, \xi)^{-1}) d\xi \end{aligned} \quad (47)$$

Then, define:

$$\begin{aligned} \psi^*(r) &= \frac{1}{2\pi} \int_{-\infty}^{\infty} \Omega_{\xi}^{-1} e^{i\xi r} d\xi \\ \Omega_{\xi} &= -(\xi V + \omega_0)^2 + 2k(\xi V + \omega_0)i + (\alpha\xi^4 + \beta)/\gamma \end{aligned} \quad (48)$$

Using this definition we can see that:

$$f^*(r) = \text{Re}[\psi^*(r)] \quad (49)$$

$$g^*(r) = \lim_{L \rightarrow \infty} g(r) = \text{Im}[\psi^*(r)] \quad (50)$$

Notice that 48 is just the definition of an inverse fourier transform of Ω_{ξ}^{-1} . We can study the zeros of this transfer function. For this purpose we can write the poles/zeros form of the fourier

transform as:

$$\begin{aligned}
\Omega_\xi &= -(\xi V + \omega_0)^2 + 2k(\xi V + \omega_0)i + (\alpha\xi^4 + \beta)/\gamma & (51) \\
&= \alpha/\gamma\xi^4 - V^2\xi^2 + (-2\omega_0V + 2kVi)\xi + (\beta/\gamma - \omega_0^2 + 2k\omega_0i) \\
&= \alpha/\gamma(i\xi)^4 + V^2(i\xi)^2 + (2\omega_0Vi + 2kV)(i\xi) + (\beta/\gamma - \omega_0^2 + 2k\omega_0i) \\
&= \alpha/\gamma s^4 + V^2s^2 + (2\omega_0Vi + 2kV)s + (\beta/\gamma - \omega_0^2 + 2k\omega_0i)
\end{aligned}$$

(c) For the fixed excitation case, we can start at equation (37) and compute the solution to the fixed excitation $F(x, t) = F\delta(t - t_0)\delta(x - x_0)$ applied at the point x_0 at time t_0 .

$$\ddot{Y}_m + 2\kappa\gamma^{-1}\dot{Y}_m + (\alpha(\pi m/L)^4 + \beta)\gamma^{-1}Y_m = F_0\delta(t - t_0)\sin(\pi mx_0/L) \quad (52)$$

Using the same definitions and initial conditions as in the moving excitation case, we can solve the above ODE:

$$Y_m(t) = F_0\Omega_m^{-1}e^{-k(t-t_0)}\sin(\Omega_m(t-t_0))\sin(\pi mx_0/L)u(t-t_0) \quad (53)$$

$$y(x, t) = \frac{2}{L}\sum_{m=0}^{\infty}Y_m(t)\sin\left(\frac{\pi mx}{L}\right) \quad (54)$$

We can develop the previous result, obtaining equation (12).

7.2 Theorem 3.2

Integrating by parts and taking into account the boundary conditions (15) at $x = 0$ and those at $x = \infty$, we get the next relations

$$\int_0^\infty y''''(x, t)\sin(\xi x)dx = -\xi^2\int_0^\infty y''(x, t)\sin(\xi x)dx = \xi^4\int_0^\infty y(x, t)\sin(\xi x)dx \quad (55)$$

These will be used as follows. We multiply both sides of equation (1) by $(2/\pi)^{1/2}\sin \xi x$ and integrate them from 0 to ∞ in x . Further on, denoting $EI = \alpha$ and dividing both parts by γ , we come to equation

$$\ddot{Y}_\xi + 2\kappa\gamma^{-1}\dot{Y}_\xi + (\alpha\xi^4 + \beta)\gamma^{-1}Y_\xi = F\gamma^{-1}\cos \omega_0 t \sin \xi V t \quad (56)$$

with initial condition $Y_\xi(0) = \dot{Y}_\xi(0) = 0$. Here

$$Y_\xi(t) = (2/\pi)^{1/2}\int_0^\infty y(x, t)\sin(\xi x)dx \quad (57)$$

is the *Fourier sine transformation* of function $y(x, t)$. The right-hand side arrived through formula

$$\int_0^\infty F\cos \omega_0(t)\sin(\xi x)\delta(x - Vt)dx = F\cos \omega_0 t \sin \xi V t \quad (58)$$

Denoting $\kappa/\gamma = k$, $(\alpha\xi^4 + \beta)/\gamma = \omega^2$, $\Omega^2 = \omega^2 - k^2$ we come to equation

$$\ddot{Y}_\xi + 2k\dot{Y}_\xi + \omega^2 Y_\xi = F_0 \cos \omega_0 t \sin \xi V t \quad (59)$$

with zero initial conditions.

Assuming $\omega^2 - k^2 > 0$, the roots of its characteristic equation are

$$\lambda = -k\xi \pm i\Omega\xi \quad (60)$$

Now we can follow the steps of Theorem 3.1 and using the definition of inverse Sine Transform in 17, we obtain Theorem 3.2.

7.3 Theorem 4.1

Denote $h(t, x^* | \omega_0, V, \phi, t_0)$ by $h(t, x^*)$. To prove (a), notice that:

$$z(t) = F h(t, x^*) + \xi(t)$$

Now, consider the the projection operator that projects $z(t)$ into two subspaces: the subspace defined by $\frac{h(t, x^*)}{\|h(t, x^*)\|}$ and the subspace orthogonal to it. It is clear that the projection to the orthogonal subspace will not contain any information about F , as the noise is white. Thus our infinite dimensional estimation problem is reduced to:

$$\int_0^\infty \frac{z(t)h(t, x^*)}{\|h(t, x^*)\|} dt = F \|h(t, x^*)\| + \int_0^\infty \frac{\xi(t)h(t, x^*)}{\|h(t, x^*)\|} dt$$

In this one dimensional problem, with a single measurement, it is clear that the optimal estimate of F is obtained by dividing both sides by $\|h(t, x^*)\|$. The MSE can be computed directly from the definition, using $\mathbb{E}[\int_0^\infty \frac{\xi(t)h(t, x^*)}{\|h(t, x^*)\|^2} dt] = 0$ and $\mathbb{E}[\int_0^\infty \frac{\xi(t)h(t, x^*)}{\|h(t, x^*)\|^2} dt]^2 = \sigma^2 / \|h(t, x^*)\|^2$ since $\xi(t)$ is white noise with variance σ^2 .

For (b) the proof follows from (a), noticing that the multiple sensor problem can be reduced to the single problem by considering a composite vector $\mathbf{z} = [z_1 z_2 \dots z_I]^T$.

The proof for (c) uses the Parseval's relation [21] for a function $f(t)$. Let $F(w)$ be the Fourier transform of $f(t)$. Then, using the time shift property of the Fourier Transform, $f(t - t_0) \Leftrightarrow e^{-j w t_0} F(w)$, and Parseval's relation, we have the identity

$$\begin{aligned} \int_0^\infty f(t - t_0)^2 dt &= \frac{1}{2\pi} \int_0^\infty |e^{-j w t_0} F(w)|^2 dw = \frac{1}{2\pi} \int_0^\infty |F(w)|^2 dw \\ &= \int_0^\infty f(t)^2 dt \end{aligned}$$

Using the identity, it is clear that for the given information set the proposed estimator computes F exactly when the measurement is noise free.

For item (e), we start by writing the empirical mean squared error function:

$$E = \int_0^\infty (z(t) - F h(t, x^* | \omega_0, V, \phi, t_0))^2 dt.$$

One of the optimality conditions for the estimator is that $\partial E / \partial F = 0$, which implies:

$$F = \frac{\sum_{i=1}^I \int_0^\infty z(t) h(t, x^* | \omega_0, V, \phi, t_0) dt}{\sum_{i=1}^I \|h(t, x^* | \omega_0, V, \phi, t_0)\|^2}.$$

Now use this equation in the definition of the error E , and ignoring the term that only depends on z , we obtain

$$E' = - \frac{(\int_0^\infty z(t) h(t, x^* | \omega_0, V, \phi, t_0) dt)^2}{\|h(t, x^* | \omega_0, V, \phi, t_0)\|^2},$$

and so maximizing $-E'$ is equivalent to minimizing E . Item (f) follows by using the same approach to the cost

$$E = \sum_{i=1}^I \int_0^\infty (z(t) - F h(t, x_i^* | \omega_0, V, \phi, t_0))^2 dt.$$

8 Discussion

In this paper we have developed a methodology for estimating the magnitude of a dynamic forcing function applied to a concrete roadway, using distributed measurements from acceleration sensors embedded in the pavement. We use an asymptotic approximation to the pavement model that can be efficiently computed as the basis of our estimator. The asymptotic model is accurate for concrete slabs starting at 20 meters.

We verified the behavior of the pavement response using some simulations and then developed a time synchronized estimator for the forcing parameter. We also calculate an error bound that shows the quality of our approximation, which is helpful to gauge the quality of responses in field experiments.

One important issue that is addressed is also the need for a maximum distance between the sensors, which we derive using principles from sampling theory. This distance is the only constraint in sensor placement for our problem.

An extension of the current model, left for future works, is to model the roadway as a 2-dimensional system. We also are in the process of validating our setup experimentally with a sensor deployed at a concrete roadway.

References

- [1] J. BAUMEISTER, W. SCONDO, M. A. DEMETRIOU, AND I. G. ROSEN, *On-line parameter*

- estimation for infinite-dimensional dynamical systems*, SIAM Journal on Control and Optimization, (1997), pp. 678–713.
- [2] D. CEBON, *Handbook of Vehicle-Road Interaction*, Swets and Zeitlinger Publishers, 1999.
- [3] T. H. T. CHAN, S. S. LAW, AND T. H. YUNG, *Interpretive method for moving force identification*, Journal of Sound and Vibration, 219 (1999), pp. 503–524.
- [4] K. CHATTI AND K. K. YUN, *Sapsi-m: Computer program for analyzing asphalt concrete pavements under moving arbitrary loads*, Transportation Research Record, (1996), pp. 88–95.
- [5] Y. CHEN, C. A. TANB, L. A. BERGMANC, AND T. C. TSAOD, *Smart suspension systems for bridge-friendly vehicles*, in Proceedings of the 2002 SPIE Annual International Symposium on Smart Structures and Materials; Smart Systems for Bridges, Structures, and Highways, 2002.
- [6] R. E. EWING, T. LIN, AND Y. LIN, *A mixed least-squares method for an inverse problem of a nonlinear beam equation*, Inverse Problems, (1999), pp. 19–32.
- [7] L. FRYBA, *Vibration of Solids and Structures under Moving Loads*, Noordhoff International Publishing, Groningen, The Netherlands, 1972.
- [8] T. T. FU AND D. CEBON, *Analysis of a truck suspension database*, Int. Journal of Heavy Vehicle Systems, 19 (2002), pp. 281–297.
- [9] M. GERDIN, T. B. SCHON, T. GLAD, F. GUSTAFSSON, AND L. LJUNG, *On parameter and state estimation for linear differential algebraic equations*, Automatica, (2007), pp. 416–425.
- [10] A. GONZALEZ, A. T. PAPAGIANNAKIS, AND E. J. O’BIEN, *Evaluation of an artificial neural network technique applied to multiple-sensor weigh-in-motion systems*, Transportation Research Record, (2003), pp. 151–159.
- [11] G. GRIMMETT AND D. STIRZAKER, *Probability and random processes*, Oxford Science Publications, Clarendon Press, Oxford, 1992.
- [12] M. S. A. HARDY AND D. CEBON, *Response of continuous pavements to moving dynamic loads*, Journal of Engineering Mechanics, (1993), pp. 1762–1780.
- [13] ———, *Importance of speed and frequency in flexible pavement response*, Journal of Engineering Mechanics, (1994), pp. 463–482.
- [14] M. H. HAYES, *Statistical Digital Signal Processing and Modeling*, John Wiley and Sons, 1996.
- [15] J. T. KENNEY, *Steady state vibrations of beam on elastic subgrade for moving loads*, Journal of Applied Mechanics, 21.
- [16] S. K. LEMING AND H. L. STALFORD, *Bridge weighin-motion system development using superposition of dynamic truck/ static bridge interaction*, in Proceedings of the American Control Conference, 2003.

- [17] L. LJUNG, *System Identification: Theory for the User*, Prentice-Hall, 2nd ed., 1999.
- [18] M. MARKOW, J. K. HEDRIC, B. D. BRADMEYER, AND E. ABBO, *Analyzing the interactions between vehicle loads and highway pavements*, in Proceedings of 67th Annual Meeting, Transportation Research Board, 1988.
- [19] F. MOSES, *Weigh-in-motion system using instrumented bridges*, Transportation Engineering Journal, 105, pp. 233–249.
- [20] A. V. . OPPENHEIM, R. W. SCHAFER, AND J. R. BUCK, *Discrete-Time Signal Processing*, Prentice-Hall, 2nd ed., 1999.
- [21] A. V. OPPENHEIM, A. S. WILLSKY, AND S. HAMID, *Signal and Systems*, Prentice-Hall, 2nd ed., 1997.
- [22] S. S. RAO, *Vibration of Continuous Systems*, John Wiley and Sons, 2007.
- [23] J. B. SOUSA, J. LYSMER, S. S. CHEN, AND C. L. MONISMITH, *Dynamic loads: effects on the performance of asphalt concrete pavements*, in Proceedings of 67th Annual Meeting, Transportation Research Board, 1988.
- [24] L. K. STERGIOULAS, D. CEBON, AND M. D. MACLEOD, *Static weight estimation and system design for multiple-sensor weigh-in-motion*, Journal Proceedings of the Institution of Mechanical Engineers, Part C: Journal of Mechanical Engineering Science, 214 (2000).
- [25] L. SUN AND T. W. KENNEDY, *Spectral analysis and parametric study of stochastic pavement loads*, Journal of Engineering Mechanics, (2002), pp. 318–327.